THE JOURNAL OF NAVIGATION (2017), **70**, 1253–1266.
doi:10.1017/S0373463317000273

Tightly Combined BeiDou B2 and Galileo E5b Signals for Precise Relative Positioning

Mingkui Wu[1], Xiaohong Zhang[1,2,3], Wanke Liu[1,2,3], Shaojie Ni[4] and Shun Yu[1]

[1](*School of Geodesy and Geomatics, Wuhan University, 129 Luoyu Road, Wuhan, 430079, P.R. China*)
[2](*Collaborative Innovation Centre for Geospatial Technology, 129 Luoyu Road, Wuhan, 430079, P.R. China*)
[3](*Key Laboratory of Geospace Environment and Geodesy, Ministry of Education, Wuhan University, Wuhan, 430079, P.R. China*)
[4](*Satellite Navigation Engineering Research Center, National University of Defense Technology, 190 Deya Road, Changsha, 410073, P.R. China*)
(E-mail: wkliu@sgg.whu.edu.cn)

In precise relative positioning applications, an effective approach to improve the interoperability of GNSS systems is the tightly combining or inter-system double-differencing of observations from the common frequencies that are shared by different constellations. As the BeiDou satellites are currently transmitting a B2 signal at 1207.14 MHz that is identical to the Galileo E5b signal, the inter-system double-differenced observations can also be created between observations from both systems at that particular frequency. In this paper, we will focus on the instantaneous ambiguity resolution performance analysis of tightly combining BeiDou B2 and Galileo E5b observations. The size and stability of phase and code Differential Inter-System Biases (DISBs) between BeiDou B2 and Galileo E5b signals are first investigated, in which the new BeiDou and Galileo satellites launched recently will also be included. Then, first results of the Tightly Combined Model (TCM) with *a priori* corrected DISBs (TCM_C) are evaluated in comparison to the Loosely Combined Model (LCM) and tightly combined model with unknown DISBs (TCM_F) in an instantaneous approach. It is demonstrated that the instantaneous integer ambiguity resolution performance can be improved using the TCM_C with respect to LCM and TCM_F.

KEYWORDS

1. BeiDou (BDS). 2. Galileo. 3. Tightly combined. 4. Differential Inter-System Bias (DISB). 5. Relative positioning.

Submitted: 28 July 2016. Accepted: 10 April 2017. First published online: 21 June 2017.

1. INTRODUCTION. With the modernisation or development of global and regional Global Navigation Satellite Systems (GNSS), many more satellites and frequencies are becoming available that provide new opportunities and challenges for high-precision relative positioning applications (Odolinski et al., 2015; Lau et al., 2015; Quan et al., 2016). In this context, interoperability of GNSS is becoming a major concern in the international satellite navigation and positioning field. A very important aspect of interoperability is the combined processing of observations from two or more GNSS systems to provide better performance at the user level (Gibbons, 2011). In precise relative positioning applications, an effective approach to improve the interoperability of GNSS systems is the tightly combined or inter-system double-differencing of observations from the common frequencies that are shared by different constellations (Julien et al., 2003). In that case, a single-pivot satellite is chosen for all the observations from different constellations. As a result, additional Double-Differenced (DD) observations can be created between the pivot satellites of each system. This extra link between the two systems strengthens the adjustment model. Compared to the loosely combined or classical double-differencing of observations from each system independently, improved performance is expected in terms of integer ambiguity resolution and position estimation (Odijk and Teunissen, 2013a; Paziewski and Wielgosz, 2015; Odijk et al., 2017; Liu et al., 2017).

However, when this approach is introduced, one must consider the between-receiver Differential Inter-System Biases (DISBs), despite the signals being tracked on the same frequency (Hegarty et al., 2004). The DISB is the difference between the hardware delays in the receiver that the signals of different GNSS systems experience and is present both in the carrier phase and code data (Montenbruck et al., 2011). The DISBs are also different in phase and code. Fortunately, when GNSS systems with overlapping frequencies are applied, the DISBs are absent for baselines with receivers of the same type; and for baselines with different receiver types, the DISBs are very stable in the time domain and thus can be calibrated *a priori* (Odijk and Teunissen, 2013a; Paziewski and Wielgosz, 2015).

Currently, most studies only focus on tightly combined relative positioning using observations from the common frequencies between Global Positioning System (GPS), Galileo, Quasi-Zenith Satellite System (QZSS) and Indian Regional Navigation Satellite System (IRNSS) (namely L1/E1 and L5/E5a). The results demonstrated that improved ambiguity resolution can be obtained with calibrated DISBs (Odijk and Teunissen, 2013a; Paziewski and Wielgosz, 2015; Odolinski et al., 2015; Odijk et al., 2017). Only a few researchers have mentioned their DISB estimation results between BeiDou (BDS) satellites and Galileo In-Orbit-Validation (IOV) satellites and none have focused on the model and performance evaluation of tightly combined relative positioning of BDS with other systems (Odijk and Teunissen, 2013b; Yuan and Zhang, 2014). As an aspect of evaluating the interoperability of BDS with other systems, this contribution will evaluate whether tightly combined precise relative positioning can also be employed between BDS and Galileo, and how well it performs. As the BDS satellites only transmit a B2 frequency at 1207.14 MHz that is identical to the Galileo E5b signal, this research is restricted to observations from BDS B2 and Galileo E5b signals. This research will provide results of tightly combined precise relative positioning of BDS and Galileo in comparison to the loosely combined positioning. Moreover, this research is also motivated by the recent launches of BDS and Galileo satellites. China launched several new-generation satellites into the BDS constellation from March 2015 to February 2016. By the end of 2015, eight Galileo Full Operational Capability (FOC) satellites were also launched into the constellation. These new satellites will also be

https://doi.org/10.1017/S0373463317000273 Published online by Cambridge University Press

included in the analysis. Furthermore, the new-generation BDS satellites will also broadcast some new signals similar to the GPS L1 and L5 signals (Xiao et al., 2016), which means that inter-system double-differencing can also be made using observations from these signals between BDS and other systems such as GPS, Galileo, and QZSS. Consequently, this paper will also provide a valuable reference for tightly combining new-generation BDS with GPS, Galileo and QZSS for precise relative positioning.

In this paper, we first demonstrate the Loosely Combined Model (LCM) and Tightly Combined Model (TCM) using observations from BDS B2 and Galileo E5b signals. The size and stability of DISBs between BDS B2 and Galileo E5b signals of all the available satellites are then investigated, using zero baseline datasets collected at Wuhan University and Curtin University. The phase and code DISBs of BDS with respect to Galileo are indeed shown to be absent for baselines with identical receiver types. For baselines with different receiver types, the phase and code DISBs are quite stable in the time domain, which gives rise to calibration of these DISBs. Finally, the performance of the TCM with *a priori* corrected DISBs (TCM_C) is evaluated with respect to the LCM and TCM model with unknown DISBs (TCM_F) based on short baseline datasets in an instantaneous approach. It is demonstrated that the instantaneous integer ambiguity resolution performance can be improved using TCM_C with respect to LCM and TCM_F.

2. MODELS FOR COMBINED BDS B2 AND GALILEO E5B RELETIVE POSITIONING.

In this section, we will present the DD observation equations corresponding to LCM, TCM_F, and TCM_C for precise relative positioning using BDS B2 and Galileo E5b signals. When DD observations are created, the satellite-specific errors and the receiver-specific errors can be eliminated. As our research is only performed for zero or short baselines, the atmospheric delays, including the ionospheric delays and tropospheric delays, can also be ignored.

2.1. *LCM using BDS B2 and Galileo E5b signals.*

When LCM is considered, one satellite is defined as the pivot satellite for BDS and Galileo respectively. Consequently, the phase and code hardware delay in the receiver can further be eliminated. The DD observation equations corresponding to LCM with 1_B as a pivot satellite for BDS and 1_E as a pivot satellite for Galileo is given by the following:

$$\begin{aligned}
\phi_{kl}^{1_B i_B} &= \rho_{kl}^{1_B i_B} + \lambda \cdot N_{kl}^{1_B i_B} + \varepsilon_{kl}^{1_B i_B} \\
\phi_{kl}^{1_E j_E} &= \rho_{kl}^{1_E j_E} + \lambda \cdot N_{kl}^{1_E j_E} + \varepsilon_{kl}^{1_E j_E} \\
P_{kl}^{1_B i_B} &= \rho_{kl}^{1_B i_B} + e_{kl}^{1_B i_B} \\
P_{kl}^{1_E j_E} &= \rho_{kl}^{1_E j_E} + \varepsilon_{kl}^{1_E j_E}
\end{aligned} \tag{1}$$

where k and l denote the receivers, i_B and j_E are the BDS and Galileo satellites respectively, ϕ is the phase observable, P is the code observable, λ is the wavelength for BDS B2 or Galileo E5b signal, ρ is the geometric range between the receiver and the satellite, N is the integer phase ambiguity, and ε and e are the phase and code measurement noise, respectively. In LCM, all of the DD observations of each system are functionally independent and the only common parameters between both systems are the baseline components.

2.2. *TCM_F using BDS B2 and Galileo E5b signals.*

When tightly combining is considered, a single pivot satellite is chosen for both systems. In that case, the phase and code

https://doi.org/10.1017/S0373463317000273 Published online by Cambridge University Press

hardware delay in the receiver cannot be eliminated. The DD observation equations corresponding to TCM_F with 1_B as pivot satellite can be given as follows (Odijk and Teunissen, 2013a; Paziewski and Wielgosz, 2015):

$$\begin{aligned}
\phi_{kl}^{1_B i_B} &= \rho_{kl}^{1_B i_B} + \lambda \cdot N_{kl}^{1_B i_B} + \varepsilon_{kl}^{1_B i_B} \\
\phi_{kl}^{1_B j_E} &= \rho_{kl}^{1_B j_E} + \lambda \cdot N_{kl}^{1_E j_E} + \lambda \cdot \tilde{\delta}_{kl}^{BE} + \varepsilon_{kl}^{1_B j_E} \\
P_{kl}^{1_B i_B} &= \rho_{kl}^{1_B i_B} + e_{kl}^{1_B i_B} \\
P_{kl}^{1_B j_E} &= \rho_{kl}^{1_B j_E} + d_{kl}^{BE} + e_{kl}^{1_B j_E}
\end{aligned} \tag{2}$$

where d_{kl}^{BE} denotes the code DISB parameter, $\tilde{\delta}_{kl}^{BE} = N_{kl}^{1_B 1_E} + \delta_{kl}^{BE}$ the lumped phase DISB parameter, which is composed of the differential phase DISB parameter (δ_{kl}^{BE}) and the ambiguity of the Galileo-pivot satellite with respect to the BDS-pivot satellite. The DISB parameters can be estimated epoch-by-epoch according to Equation (2).

Although the code DISB is an unbiased parameter, the estimable phase DISB parameter ($\tilde{\delta}_{kl}^{BE}$) is biased by the inter-system ambiguity between the pivot satellites ($N_{kl}^{1_B 1_E}$). As a result, the phase DISB is obtained by taking the fractional part of the estimated lumped phase DISB parameter in this paper. Moreover, compared to the LCM, the increase in the number of observations is equal to the increase in the number of unknowns for this model. This means that the single-epoch TCM_F does not contribute to the model strength. As a result, identical performance is expected using this model with respect to the LCM.

2.3. *TCM_C using BDS B2 and Galileo E5b signals.* As the DISBs are very stable in the time domain, the adjustment model can be strengthened by *a priori* DISB calibration and correction. According to Equation (2), the phase and code DD observations corresponding to TCM_C then become the following (Odijk and Teunissen, 2013a; Paziewski and Wielgosz, 2015):

$$\begin{aligned}
\phi_{kl}^{1_B i_B} &= \rho_{kl}^{1_B i_B} + \lambda \cdot N_{kl}^{1_B i_B} + \varepsilon_{kl}^{1_B i_B} \\
\tilde{\phi}_{kl}^{1_B j_E} &= \rho_{kl}^{1_B j_E} + \lambda \cdot N_{kl}^{1_B j_E} + \varepsilon_{kl}^{1_B j_E} \\
P_{kl}^{1_B i_B} &= \rho_{kl}^{1_B i_B} + e_{kl}^{1_B i_B} \\
\tilde{P}_{kl}^{1_B j_E} &= \rho_{kl}^{1_B j_E} + e_{kl}^{1_B j_E}
\end{aligned} \tag{3}$$

where $\tilde{P}_{kl}^{1_B j_E}$ denotes DD code observation with code DISB corrected, and $\tilde{\phi}_{kl}^{1_B j_E}$ is the DD phase observation with phase DISB corrected. Note that it is sufficient to use the fractional part of phase DISB to correct phase observations, because the integer part of the phase DISB can be lumped with the corresponding inter-system DD integer ambiguities without affecting integer ambiguity resolution and positioning (Odijk and Teunissen, 2013a; Paziewski and Wielgosz, 2015).

The model strength of the TCM_C is stronger in comparison to the TCM_F or LCM. The redundancy is increased by one per epoch compared to LCM and TCM_F. As a result, improved performance is expected theoretically using the TCM_C with respect to LCM and TCM_F.

3. RESULTS OF DISB ESTIMATION AND THEIR IMPACT ON AMBIGUITY RESOLUTION.

In this section, we will analyse phase and code DISBs between the BDS B2

https://doi.org/10.1017/S0373463317000273 Published online by Cambridge University Press

and Galileo E5b signals from zero baseline datasets collected at Wuhan University and Curtin University. Identical and different types of geodetic multi-GNSS receivers are used in the Wuhan University experiment and Curtin University experiment respectively. We will determine phase and code DISBs based on the observation model in Equation (2). The DISBs are estimated epoch-by-epoch with known receiver positions under 10° elevation cut-off angle.

The estimated DISBs for BDS B2 and Galileo E5b signals are then applied to another dataset with a short baseline, in order to investigate the impact of DISBs on ambiguity resolution. The performance of the TCM_C will be evaluated in comparison to the LCM and TCM_F. In TCM_C, the phase and code DISBs between BDS B2 and Galileo E5b signals are *a priori* corrected and the positioning is conducted according to Equation (3). Conversely, in TCM_F, the phase and code DISBs are estimated according to Equation (2). In the data processing procedure, the position estimation and integer estimation is conducted epoch-by-epoch. The empirical success rate (P_{se}) and the empirical failure rate (P_{fe}) are used to verify the performance of ambiguity resolution, which are defined as (Odolinski et al., 2014):

$$P_{se} = \frac{\#\text{accepted and correctly fixed epochs}}{\text{total \# of epochs}} \tag{4}$$

$$P_{fe} = \frac{\#\text{accepted and incorrectly fixed epochs}}{\text{total \# of epochs}} \tag{5}$$

Whether the ambiguities are correctly fixed in a certain epoch is determined by comparing the estimated ambiguities to the true ambiguities, which are solved using all of the available multi-system and multi-frequency observations over the whole time span. Note that the Least-squares AMBiguity Decorrelation Adjustment (LAMBDA) method is used for ambiguity resolution and the Fixed Critical-value Ratio Test (FCRT) as well as the Fixed Failure-rate Ratio Test (FFRT) are used for ambiguity validation (Teunissen and Verhagen, 2009; Verhagen and Teunissen, 2013). We set the corresponding FCRT to standard values of 1/2 and 1/3, and FFRT with user-defined failure rate (P_f) of 1% and 0·1% respectively.

It should be noted that as Galileo satellites E14 and E18 were originally injected in an anomalous orbit (Hellemans, 2014), there are no broadcast ephemerides available for these two satellites. Therefore, a precise orbit and clock product from the Multi-GNSS Experiment (MGEX) of the International GNSS Service (IGS) are used for Galileo. On the other hand, the broadcast ephemerides are used for BDS.

3.1. *Experiments with Identical Receiver Type at Wuhan University.* Two datasets including a zero baseline experiment and a short baseline experiment, were collected on the roof of School of Geodesy and Geomatics (SGG) at Wuhan University. Two identical prototype receivers developed by a university in China, and two identical TRM59900·00 NONE antennae were used in the experiments. The zero baseline experiment (two receivers connected to a TRM59900·00 NONE antenna) was conducted on 13 May 2016 (from 00:00 to 24:00 GPST) and used for DISB estimation. The short baseline (separated by 3.28 m) experiment was conducted on 16 May 2016 (from 04:00 to 24:00 GPST) and used to investigate the impact of DISB on ambiguity resolution. The observations were collected with 10 s sampling interval and 10° elevation cut-off angle. The observation conditions and GNSS antennae used in zero and short baseline experiments are shown in Figure 1.

https://doi.org/10.1017/S0373463317000273 Published online by Cambridge University Press

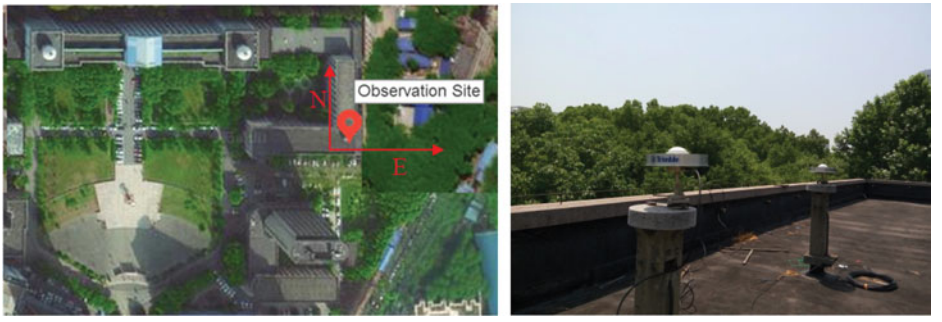

Figure 1. Observation conditions and GNSS antennae used in zero and short baseline experiments at SGG of Wuhan University.

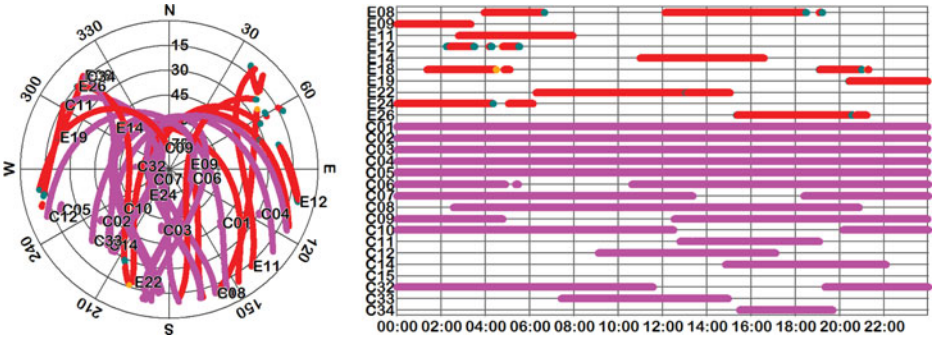

Figure 2. Sky plot (left) and availability (right) of BDS and Galileo satellites on 13 May 2016, above 10° elevation cut-off angle.

3.1.1. *DISB Estimation of Identical Receivers with Zero Baseline Experiment.* Figure 2 depicts the sky plot and the availability of BDS and Galileo satellites during 13 May 2016, above a 10° elevation cut-off angle. As shown, three newly launched BDS satellites (namely C32, C33, and C34) can be observed during the day. However, only one newly launched BDS satellite can be observed for most of the time span.

Figure 3 (left) shows the number of BDS and Galileo satellites tracked above a 10° elevation cut-off angle. Figure 3 (left) shows that the number of BDS satellites varies between nine and 12, whereas the number of Galileo satellites varies between one and five. Figure 3 (right) shows that the phase and code DISB series are both fairly stable in the time domain. Moreover, the mean of these DISBs over the day are close to zero (−0·005 cycles and 0·014 m), as is expected for a pair of identical receivers. The estimated phase and code DISBs also show a much noisier behaviour around 04:00, 12:00, and 20:00 GPST due to the low elevation of Galileo satellites at these times.

3.1.2. *Impact of DISB on Ambiguity Resolution with Short Baseline Experiment.* The data were collected from 04:00 to 24:00 GPST, 16 May 2016, which is separated by three days from the previous zero baseline experiment. The sky plot and availability of BDS and Galileo satellites are shown in Figure 4. As shown, three newly launched BDS satellites (namely C32, C33, and C34) can also be observed during the day. Two newly launched BDS satellites can be tracked from 04:00 to 09:20 GPST and 19:10 to 19:50 GPST, while

https://doi.org/10.1017/S0373463317000273 Published online by Cambridge University Press

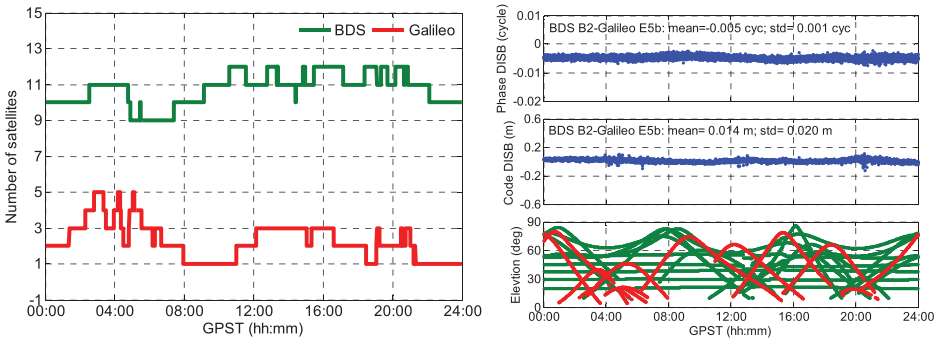

Figure 3. Number of BDS and Galileo satellites tracked on 13 May 2016, above a 10° elevation cut-off angle (left) versus estimated DISBs between BDS and Galileo (right) for zero baseline based on identical receivers. The phase DISB is shown in the upper graph, the code DISB in the middle graph, and the elevations in the bottom graph (red: Galileo; green: BDS).

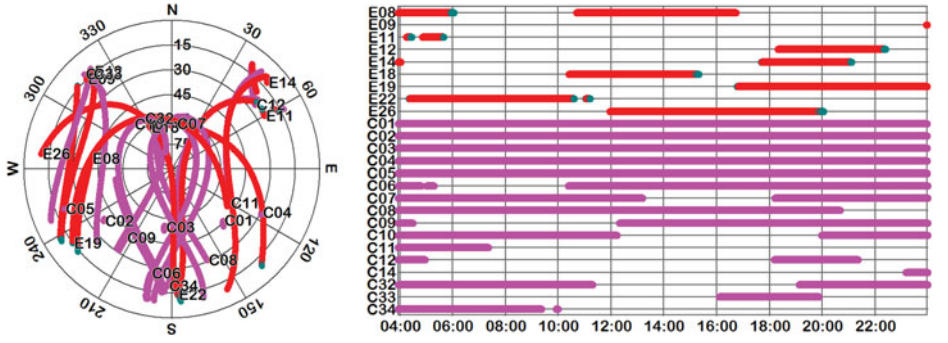

Figure 4. Sky plot (left) and availability (right) of BDS and Galileo satellites on 16 May 2016, above a 10° elevation cut-off angle.

from 11:20 to16:00 GPST, no newly launched BDS satellites are available. The number of satellites and PDOP for BDS and Galileo satellites are shown in Figure 5 (left). Figure 5 (left) shows that the number of available BDS satellites is no less than eight for most of the time span and can even reach up to 14 due to the addition of the newly launched BDS satellites; while the number of available Galileo satellites is no less than one for most of the time span and can reach up to four. When combining BDS with Galileo, the number of available satellites is no less than nine for most of time span and can even reach up to 17.

Figure 5 (right) shows the epoch-by-epoch Ambiguity Dilution of Precision (ADOP) (Teunissen et al., 2014) and bootstrapped success rate (BSR) (Teunissen, 1998) time series for LCM, TCM_F, and TCM_C. Note that as shown in the zero baseline experiment, the phase and code DISBs (−0·005 cycles and 0·014 m) are close to zero and falling within the precision level of a few mm and dm for an un-differenced phase and code observations, they are regarded as absent and are ignored in the TCM_C. As the single epoch ADOP time series of TCM_F is identical to that of LCM, the ADOP time series of TCM_F is not visible in the figure. This is also in line with the theoretical analysis in the "TCM_F using BDS B2 and Galileo E5b signals" section. On the other hand, the single epoch ADOP time series of TCM_C is obviously smaller than LCM and TCM_F, which is due to the

https://doi.org/10.1017/S0373463317000273 Published online by Cambridge University Press

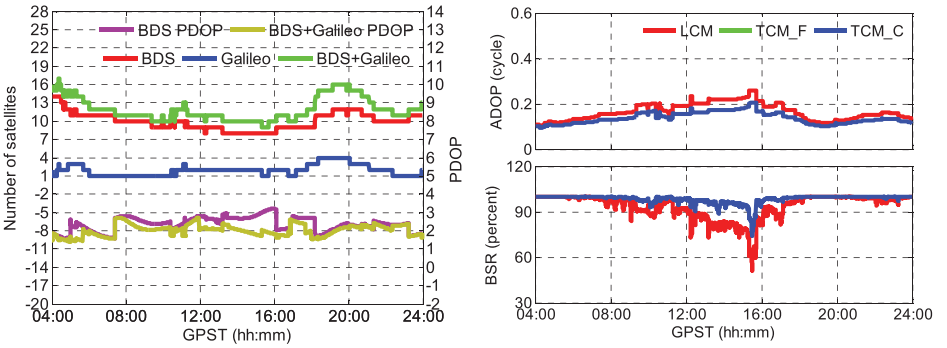

Figure 5. Number of satellites and PDOP (left), ADOP and BSR (right) on 16 May 2016, above a10° elevation cut-off angle.

Table 1. Empirical success rate and failure rate (percent) with FCRT $u = 1/2$, $u = 1/3$, and FFRT $P_f = 1\%$, $P_f = 0{\cdot}1\%$. The second column denotes the average number of satellites used over the whole time span for LCM (TCM_F and TCM _C within brackets). Number of epochs 7,200.

Elevation Cutoff	Ave. Num. of Sat.	IAR Validation Strategy	Success rate (P_{se})			Failure rate(P_{fe})		
			LCM	TCM_F	TCM_C	LCM	TCM_F	TCM_C
10°	11·7 (12.0)	FCRT $u = 1/2$	99·31	99·31	99·61	0	0	0
		FCRT $u = 1/3$	98·50	98·50	99·25	0	0	0
		FFRT $P_f = 1\%$	99·46	99·46	99·94	0·04	0.04	0·04
		FFRT $P_f = 0{\cdot}1\%$	96·60	96·60	99·71	0·04	0·04	0
20°	10·7 (11·2)	FCRT $u = 1/2$	99·04	99·04	99·46	0·31	0·31	0
		FCRT $u = 1/3$	98·47	98·47	99·13	0·26	0·26	0
		FFRT $P_f = 1\%$	98·43	98·43	99·68	0·31	0·31	0
		FFRT $P_f = 0{\cdot}1\%$	89·54	89·54	98·56	0·10	0·10	0

increase of redundancy when the phase and code DISBs are *a priori* corrected. The mean ADOP is 0·166, 0·166, and 0·138 cycles for LCM, TCM_F, and TCM_C, respectively, while the mean BSR is 93·23%, 93.23%, and 98·43%. This means that a higher rate of integer ambiguity resolution performance can be theoretically expected for TCM_C with respect to LCM and TCM_F.

Table 1 shows the epoch-by-epoch empirical ambiguity resolution performance of LCM, TCM_F and TCM_C with four different integer validation strategies (FCRT with $u = 1/2, u = 1/3$, and FFRT with $P_f = 0{\cdot}1\%$, $P_f = 1\%$) and with 10° and 20° elevation cut-off angle. As shown, identical results are obtained using LCM and TCM_F. Conversely, the TCM_C can provide us with a much higher empirical ambiguity resolution success rate and lower empirical failure rate with respect to the LCM and TCM_F with four integer validation strategies. In the case of the 10° elevation cut-off angle, the empirical ambiguity resolution success rates of TCM_C are increased from 99·31%, 98·50%, 99·46%, and 96·60% to 99·61%, 99·25%, 99·94%, and 99·71% with respect to LCM, respectively; if the elevation cut-off angle is 20°, the empirical ambiguity resolution success rates are increased from 99·04%, 98·47%, 98·43%, and 89·54% to 99·46%, 99·13%, 99·68%, and 98·56%. The improvement is marginal with integer validation strategies of FCRT with $u = 1/2$, $u = 1/3$,

https://doi.org/10.1017/S0373463317000273 Published online by Cambridge University Press

Figure 6. Observation conditions and GNSS antennae (http://www.igs.org/images/site/CUT0_1.jpg) used in zero and short baseline experiments at Curtin University Bentley campus.

and FFRT with P_f = 1%. This is reasonable considering LCM can already deliver excellent integer ambiguity resolution results due to the good observation geometry. The improvement (approximately 9%) is most evident in the case of 20° elevation cut-off angle with the integer validation strategy of FFRT with P_f = 0·1%, which is the most rigorous integer validation strategy of the four strategies used. This means that the TCM_C is especially beneficial when the available satellites are limited under a constrained environment.

3.2. *Experiments with Different Receiver Types at Curtin University Bentley Campus.* Similarly, two datasets, including a zero baseline experiment and a short baseline experiment, were collected at Curtin University Bentley campus. The zero baseline experiment was carried out on the roof of Curtin Building 402. A Trimble NetR9 (CUT0) and a JAVAD TRE_G3TH DELTA (CUT3) were connected to a TRM59800·00 SCIS antenna in the zero baseline experiment. The zero baseline experiment was conducted on 15 September 2015 (from 00:00 to 24:00 GPST) and used for DISB estimation. Furthermore, on the roof of campus Building 207, another JAVAD TRE_G3TH DELTA receiver (SPA7) was setup and connected to a TRM59800.00 SCIS antenna as well. The short baseline (separated by approximately 357.59 m) experiment was carried out with station CUT0 and SPA7 on 16 October 2015 (from 00:00 to 24:00 GPST) and used to investigate the impact of DISB on ambiguity resolution. The observations are collected with 30 s sampling interval and 10° elevation cut-off angle. The observation conditions and GNSS antennae used in zero and short baseline experiments are shown in Figure 6.

Note that in contrast to the experiments at Wuhan University, none of the newly launched BDS satellites can be tracked by the receivers used in these experiments. Moreover, as Galileo satellites E08 and E09 were launched on 17 December 2015, these two satellites were not tracked by the receivers either. Consequently, the available satellites tracked in the experiments are fewer than those tracked in the experiments at Wuhan University.

3.2.1. *DISB Estimation of mixed Receivers with Zero Baseline Experiment.* Figure 7 depicts the sky plot and availability of BDS and Galileo satellites on 15 September 2015, above a 10° elevation cut-off angle. As shown, none of newly launched BDS satellites are tracked during the day.

https://doi.org/10.1017/S0373463317000273 Published online by Cambridge University Press

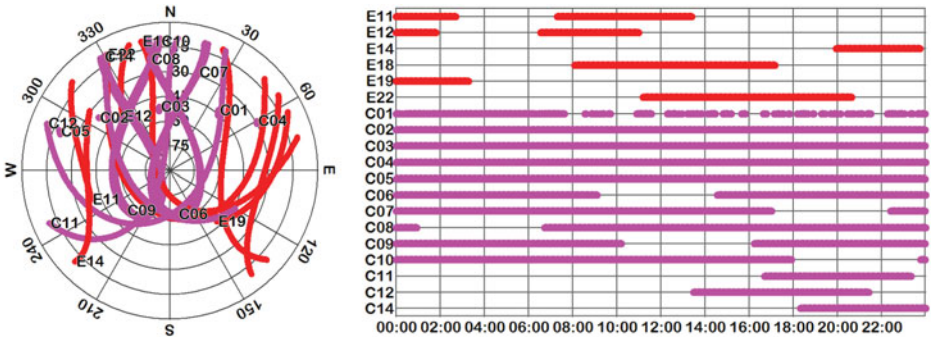

Figure 7. Sky plot (left) and availability (right) of BDS and Galileo satellites on 15 September 2015, above a 10° elevation cut-off angle.

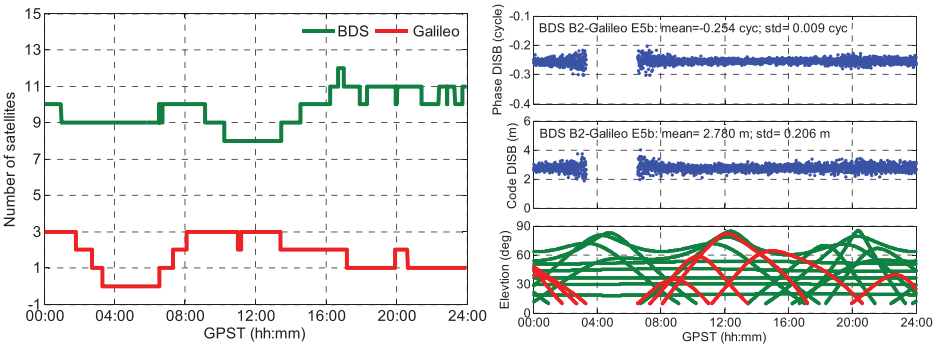

Figure 8. Number of BDS and Galileo satellites tracked on 15 September 2015, above a 10° elevation cut-off angle (left) versus estimated DISBs between BDS and Galileo satellites (right) for zero baseline based on different types of receivers. The phase DISB is shown in the upper graph, the code DISB in the middle graph, and the elevations in the bottom graph (red: Galileo; green: BDS).

Figure 8 (left) shows the number of BDS and Galileo satellites tracked above a 10° elevation cut-off angle. Figure 8 (left) shows that the number of BDS satellites varies between eight and 12, whereas the number of Galileo satellites varies between zero and three. It can be seen that both the code and phase DISB series are also fairly stable in the time domain. For this receiver combination of Trimble NetR9 and JAVAD TRE_G3TH_8 DELTA, the estimated phase and code DISBs are −0·254 cycles and 2.78 m, respectively. Additionally, there is a gap in the DISB time series from 03:18 to 06:33 GPST. This is reasonable considering that there were no Galileo satellites tracked above a 10° elevation cut-off angle during this time span. The estimated phase and code DISBs also show a much noisier behaviour around 03:00, 07:00, and 20:00 GPST due to the low elevation of Galileo satellites at these times.

3.2.2. *Impact of DISB on Ambiguity Resolution with Short Baseline Experiment.* The data were collected from 00:00 to 24:00 GPST, 16 October 2015, which is separated by one month from the previous zero baseline experiment. The sky plot and availability of BDS and Galileo satellites are shown in Figure 9. The number of satellites and PDOP for BDS and Galileo satellites are shown in Figure 10 (left). Figure 10 (left) shows that the number of available BDS satellites is no less than seven for most of the time span and can reach

https://doi.org/10.1017/S0373463317000273 Published online by Cambridge University Press

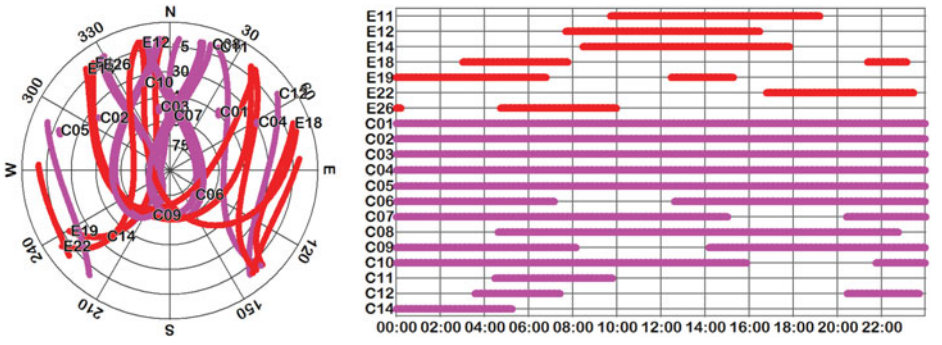

Figure 9. Sky plot and availability of BDS and Galileo satellites on 16 October 2015 above a 10° elevation cut-off angle.

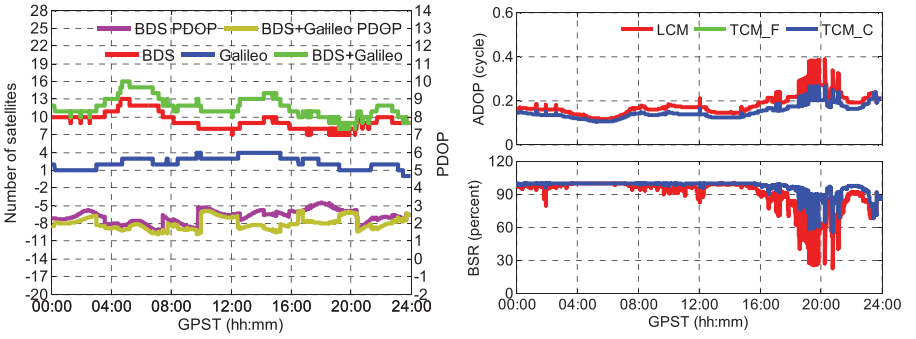

Figure 10. Number of satellites, PDOP (left), ADOP and BSR (right) on 16 October 2015, above a 10° elevation cut-off angle.

up to 13, while the number of available Galileo satellites is no less than one for most of the time span and can reach up to four. When combining BDS with Galileo, the available satellites are no less than nine for most of time span and can reach up to 16. The available satellites tracked in the experiments are fewer than those tracked in the experiments at Wuhan University due to the absence of newly launched BDS satellites and Galileo E08 and E09.

Figure 10 (right) shows the epoch-by-epoch ADOP and BSR for LCM, TCM_F, and TCM_C. Note that in TCM_C the phase and code DISBs are *a priori* calibrated to the estimated values (−0·254 cycles for phase and 2·78 m for code respectively) in the zero baseline experiment. In line with the experiments at Wuhan University, it is also demonstrated that the single epoch ADOP time series of TCM_F is identical to that of LCM and the single epoch ADOP time series of TCM_C is obviously smaller than LCM. The mean ADOP is 0·177, 0·177, and 0·147 cycles for LCM, TCM_F, and TCM_C, respectively, while the mean BSR is 90·92%, 90·92%, and 97·05%.

Table 2 shows the epoch-by-epoch empirical ambiguity resolution performance of LCM, TCM_F, and TCM_C with four different integer validation strategies and with 10° and 20° elevation cut-off angles. In line with the results in experiments at Wuhan University, the TCM_F can provide us with identical AR performance with respect to LCM. Compared to LCM and TCM_F, TCM_C also provides us with a much higher empirical ambiguity

https://doi.org/10.1017/S0373463317000273 Published online by Cambridge University Press

Table 2. Empirical success rate and failure rate (percent) with FCRT $u = 1/2$, $u = 1/3$, and FFRT $P_f = 1\%$, $P_f = 0.1\%$. The second column denotes the average number of satellites over the whole time span used for LCM (TCM_F and TCM _C within brackets). Number of epochs 2,880.

Elevation Cutoff	Ave. Num. of Sat.	IAR Validation Strategy	Success rate (P_{se})			Failure rate(P_{fe})		
			LCM	TCM_F	TCM_C	LCM	TCM_F	TCM_C
10°	11·5 (11.8)	FCRT $u = 1/2$	99·58	99·58	99·97	0	0	0
		FCRT $u = 1/3$	98·23	98·23	99·83	0	0	0
		FFRT $P_f = 1\%$	97·74	97·74	99·93	0	0	0
		FFRT $P_f = 0.1\%$	87·74	87·74	98·30	0	0	0
20°	9.3 (9.7)	FCRT $u = 1/2$	91·42	91·42	98·09	0·42	0·42	0·04
		FCRT $u = 1/3$	84·96	84·96	96·01	0·17	0·17	0.04
		FFRT $P_f = 1\%$	77·74	77·74	92·12	0	0	0·04
		FFRT $P_f = 0.1\%$	56·79	56·79	80·97	0	0	0

resolution success rate and lower empirical failure rate with four integer validation strategies. As the number of available satellites tracked in this experiment is fewer than the number tracked in the short baseline experiment at Wuhan University, the improvement of AR performance in this experiment is more significant compared to that in the experiment at Wuhan University. The improvement is most evident with a 20° elevation cut-off angle, which is approximately 8%, 13%, 14%, and even 24% with the four different integer validation strategies, respectively. The reason is that the number of available satellites for LCM is only approximately 9.3, and the observational geometry is relatively poor with a 20° elevation cut-off angle. In that case, the additional DD observations in TCM_C can bring great benefits to strengthen the adjustment model and thus deliver significant improvement to the ambiguity resolution performance. The results demonstrate that the TCM_C is especially beneficial for improving ambiguity resolution performance under constrained environments such as serious open-pit masking, satellite outages, or urban canyon, in which cases the available satellites are limited or observation geometry is poor.

4. CONCLUSIONS. In this paper, for the first time, the performance of tightly combined BDS B2 and Galileo E5b single-epoch single-frequency relative positioning has been presented in terms of ambiguity resolution. We first investigate the size and stability of DISBs between the BDS B2 and Galileo E5b signals using identical and different receiver types. For a zero baseline with receivers of the same type, it is verified that the phase and code DISBs of BDS B2 signal with respect to Galileo E5b signal are indeed absent. For a zero baseline with different receiver types, it is demonstrated that the phase and code DISBs between the BDS B2 and Galileo E5b signals are estimated as nonzero but are fairly stable in the time domain, which is in line with the DISBs for mixed receivers based on combinations of GPS, Galileo, QZSS, and IRNSS with L1/E1 and L5/E5a signals. Then, the performance of the TCM_C is evaluated with respect to the LCM and TCM_F based on short baseline datasets in an instantaneous approach. It is demonstrated that identical results are obtained using LCM and TCM_F. Conversely, the instantaneous integer ambiguity resolution performance can be improved using TCM_C with respect to LCM. In our short baseline experiments separated by approximately 3·28 m and 357·59 m, the TCM_C can deliver approximately 9% and 24% improvement of empirical integer

https://doi.org/10.1017/S0373463317000273 Published online by Cambridge University Press

resolution success rate, respectively, in the case of a 20° elevation cut-off angle with integer validation strategy of FFRT with P_f = 0·1%. The results demonstrate that the TCM_C is especially beneficial when the number of available BDS and Galileo satellites are limited under constrained environments such as serious open-pit masking, satellite outages or urban canyon, because in that case, the available satellites may be insufficient for reliable single epoch ambiguity resolution and positioning using LCM.

Real kinematic data will be used to further verify the performance of the presented approach in the future. Future research will also be carried out to evaluate the performance of tightly combined positioning of BDS with respect to other systems (GPS, Galileo and QZSS), if observations of new signals similar to that of GPS from the new-generation BDS satellites are available.

ACKNOWLEDGMENTS

This work is supported by the National Key Research and Development Plan (No. 2016YFB0501803), National Natural Science Foundation of China (No. 91638203, 41474025), and Natural Science Foundation for Distinguished Young Scholar of Hubei Province (No. 2015CFA039). The authors would also like to acknowledge the Curtin University for providing the GNSS data and the Multi-GNSS Experiment (MGEX) of the International GNSS Service (IGS) for providing precise orbit and clock products. Valuable comments from the anonymous reviewers are acknowledged as well.

REFERENCES

Gibbons, G. (2011). GNSS Interoperability. *Inside GNSS*, **6**, 28–31.

Hegarty, C., Powers, E., and Foville, B. (2004). Accounting for timing biases between GPS, modernized GPS, and Galileo signals. *Proceedings of 36th annual precise time and time interval meeting*,Washington, DC.

Hellemans, A. (2014) A simple plumbing problem sent Galileo satellites into wrong orbits. http://spectrum.ieee.org/tech-talk/aerospace/satellites/a-simple-plumbing-problem-sent-galileo-satellites-into-wrong-orbits. Accessed 13 October 2014.

Julien, O., Alves, P., Cannon, M.E., and Zhang, W. (2003). A tightly coupled GPS/GALILEO combination for improved ambiguity resolution. *Proceedings of the European Navigation Conference*(*ENC-GNSS'03*), Graz, Austria.

Lau, L., Tateshita, H., and Sato, K. (2015). Impact of Multi-GNSS on Positioning Accuracy and Multipath Errors in High-Precision Single-Epoch Solutions–A Case Study in Ningbo China. *Journal of Navigation*, **68**, 999–1017.

Liu, H., Shu, B., Xu, L., Qian, C., Zhang, R., and Zhang, M. (2017). Accounting for Inter-System Bias in DGNSS Positioning with GPS/GLONASS/BDS/Galileo. *Journal of Navigation*, 1–13.

Montenbruck, O., Hauschild, A. and Hessels, U. (2011). Characterization of GPS/GIOVE sensor stations in the CONGO network. *GPS Solutions*, **15**, 193–205.

Nadarajah, N., Khodabandeh, A. and Teunissen, P.J.G. (2015). Assessing the IRNSS L5-signal in combination with GPS, Galileo, and QZSS L5/E5a-signals for positioning and navigation. *GPS Solutions*, **20**, 289–297.

Odijk, D. and Teunissen, P.J.G. (2013a). Characterization of between receiver GPS-Galileo inter-system biases and their effect on mixed ambiguity resolution. *GPS Solutions*, **17**, 521–533.

Odijk, D. and Teunissen, P.J.G. (2013b). Estimation of differential inter-system biases between the overlapping frequencies of GPS, Galileo, BeiDou and QZSS. *Proceedings of the 4th International Colloquium Scientific and Fundamental Aspects of the Galileo Programme*, Prague, Czech Republic.

Odijk, D., Nadarajah, N., Zaminpardaz, S. and Teunissen, P.J.G. (2017). GPS, Galileo, QZSS and IRNSS differential ISBs: estimation and application. *GPS Solutions*, **21**, 439–450.

Odolinski, R., Teunissen, P.J.G. and Odijk, D. (2014). First combined COMPASS/BeiDou-2 and GPS positioning results in Australia. Part II: Single-and multiple-frequency single-baseline RTK positioning. *Journal of Spatial Science*, **59**, 25–46.

Odolinski, R., Teunissen, P.J.G. and Odijk, D. (2015). Combined BDS, Galileo, QZSS and GPS single-frequency RTK. *GPS Solutions*, **19**, 151–163.

Paziewski, J. and Wielgosz, P. (2015). Accounting for Galileo-GPS inter-system biases in precise satellite positioning. *Journal of Geodesy*, **89**, 81–93.

Quan, Y., Lau, L., Roberts, G., and Meng, X. (2016). Measurement Signal Quality Assessment on All Available and New Signals of Multi-GNSS (GPS, GLONASS, Galileo, BDS, and QZSS) with Real Data. *Journal of Navigation*, **69**, 313–334.

Teunissen, P.J.G. (1998). Success probability of integer GPS ambiguity rounding and bootstrapping. *Journal of Geodesy*, **72**, 606–612.

Teunissen, P.J.G. and Verhagen, S. (2009). The GNSS ambiguity ratio-test revisited: a better way of using it. *Survey Review*, **41**, 138–151.

Teunissen, P.J.G., Odolinski, R. and Odijk, D. (2014). Instantaneous BeiDou+GPS RTK positioning with high cut-off elevation angles. *Journal of Geodesy*, **88**, 335–350.

Verhagen, S. and Teunissen, P.J.G. (2013). The ratio test for future GNSS ambiguity resolution (2013). *GPS Solutions*, **17**, 535–548.

Xiao, W., Liu, W. and Sun, G. (2016). Modernization milestone: BeiDou M2-S initial signal analysis. *GPS Solutions*, **20**, 125–133.

Yuan, Y. and Zhang, B. (2014) Retrieval of inter-system biases (ISBs) using a network of multi-GNSS receivers. *Journal of Global Positioning System*, **13**, 22–29.